



Analysis of lymphatic metastasis and progression patterns for clinical target volume (CTV) definition in head and neck squamous cell carcinoma (HNSCC)

B. Pouymayou , C. Koechli, P. Balermipas, M. Guckenberger and J. Unkelbach

Radiation Oncology Department, University Hospital Zürich, Zurich, Switzerland

ARTICLE HISTORY Received 2 April 2019; Accepted 3 July 2019

Introduction

Treatment planning in radiotherapy distinguishes three target volume concepts: the gross tumor volume (GTV), the clinical target volume (CTV) and the planning target volume (PTV). In contrast to GTV delineation, CTV delineation is not based on contouring an abnormal mass on tomographic images but relies on knowledge of patterns of disease progression. Currently, there is a lack of mathematical methods to describe progression patterns and the risk of microscopic involvement quantitatively.

In this paper, we consider elective CTV definition (CTV-N) in head and neck squamous cell carcinoma (HNSCC) patients. HNSCC spread through the lymphatic system and form metastases in regional lymph nodes [1]. The CTV-N contains not only lymph nodes that appear abnormal on imaging, but a large portion of the lymph drainage area at risk of harboring occult metastases. To that end, the lymph drainage area is divided into anatomically defined regions called lymph nodes levels (LNL). Grégoire et al. [2] provide a precise definition of LNL in the neck for radiotherapy planning.

The risk of microscopic involvement of LNL depends on multiple factors. One important factor is the location and stage of the primary tumor (PT). This aspect is discussed in several publications [1,3–5]. In addition, the risk of occult metastases in some LNL depends on the patient's state of nodal disease progression, i.e., the location of macroscopic lymph node metastasis that is already visible on imaging. Few publications provide a quantitative analysis of this second factor. For example, the observation of macroscopic metastases in level II is expected to increase the risk of occult metastases in level III. This is in part because level III receives efferents from level II. However, to the best of our knowledge, the work by Sanguineti et al. [6] is the only published study on the number of patients in a cohort, which present with a specific combination of involved LNL. Unfortunately, other publications only report the cumulative incidence of metastatic involvement of LNL.

The overarching goal of this paper is to present a method using Bayesian statistics to estimate the probability of microscopic involvement of LNL, taking into account the location

of macroscopic metastases. To achieve this goal, the lymphatic progression patterns, i.e., the probability of tumors to spread to and between various LNL, must be modeled quantitatively. The input to such a model is a dataset of newly diagnosed HNSCC patients in which the involvement of LNLs is recorded for every patient. The remainder of this paper is organized along three contributions, leading to microscopic involvement risk estimation:

1. We publish a data set of lymphatic progression patterns in 132 HNSCC patients. The dataset is available as **Supplementary Material** in the form of a comma-separated values (CSV) file (<https://figshare.com/s/be261949f56-b9a4ce1d6>) and this paper describes this dataset.
2. Visualizing the raw data on lymphatic progression patterns is complex. Therefore, we present a graphical user interface (GUI) that allows for intuitive visualization of the dataset and for recognizing patterns in LNL involvement.
3. We outline how detailed analysis of lymphatic progression patterns may lead to personalized CTV-N definition based on the individual patient's state of disease progression. To that end, Bayesian statistics is applied.

Material and methods

Data collection

We retrospectively analyzed 132 HNSCC patients (T1–T4) treated with definitive radio- or radiochemotherapy at our institution. For each patient, we recorded the ipsi- and contralateral involved LNL (I–X) on the planning CT and when available on positron emission tomography (PET), pathology and magnetic resonance imaging (MRI) reports. A detailed presentation of the dataset can be found in the **Supplementary Material, Appendix A.1**.

Data exploration

The data collected were stored in a structured data base using the Structured Query Language (SQL) formalism (SQLite version 3.26.0, SQLite Development Team, available from <https://www.sqlite.org/download.html>). All the data

were anonymized and only referenced by a patient ID. Appendix A.2 describes the database structure. A GUI was developed to generate SQL queries and display lymphatic progression patterns in an intuitive way. The interface with the database is implemented in python and uses the Kivy graphical library to handle user interactions. The functionality of the GUI is illustrated in the results section.

From macroscopic progression patterns to risk of microscopic involvement

For patients treated with definitive radiotherapy or chemoradiotherapy, only the spatial distribution of macroscopic metastases is known. These observations can be used to estimate the risk of microscopic involvement, which depends mostly on two factors:

1. The probabilities of the PT to spread through the lymphatic network. This information is contained in the data set of progression patterns. The natural assumption is that microscopic involvement precedes macroscopic involvement and both follow the same progression patterns.
2. The sensitivity and specificity of diagnostic imaging modalities. In this work, we use published literature values of sensitivity and specificity.

The methodology of Bayesian networks (BN) [7,8] is well suited to combine these data and obtain a consistent statistical model of lymphatic progression and microscopic involvement. Mathematically, the BN calculates the conditional probabilities that a LNL is microscopically involved, given the observed macroscopic involvement for the individual patient at hand and the dataset of macroscopic tumor progression patterns. The method is in parts described in a previous publication [9]. Here, we extend this methodology toward Bayesian inference to account for model parameter uncertainty (Appendix B). We illustrate the method in the

following section by estimating the risk of microscopic involvement of level III given in the macroscopic observations of level II.

Results

Dataset description

The PTs were located in the oropharynx (84), hypopharynx (28), oral cavity (10) and larynx (10) and had rather advanced stages: T1 (9), T2 (38), T3 (31) and T4 (54). In Table 1, we report for planning CT and for the different PT locations, the number of patients with a specific configuration of involved LNL levels (considering levels I, II, III and IV). Since for central cases, ipsi- and contralateral sides are ill-defined, Table 1 considers lateralized cases only. A detailed description including PET data is presented in Appendix A.3 and the full dataset is available as Supplementary Material.

Graphical user interface

Figure 1 shows the GUI to explore the data base. Users can select any of the variables (light blue buttons, which when selected, turn dark blue) on the layout. In the example in Figure 1, the user has selected 'oropharynx' as the PT location and the '+' sign for ipsilateral LNL II. In addition, 'central' is set to '-'. Thereby, the subset of patients under consideration is restricted, to patients with lateralized PT in the oropharynx with involvement of ipsilateral level II (corresponding to 67 patients out of 84 oropharyngeal patients). Under each LNL button, the GUI displays the number of patients with involvement in this level. For example, out of the 67 patients with ipsilateral level II involvement, 23 patients had also ipsilateral level III involved.

By clicking on the LNL button itself, the user can display an additional table (Figure 1(b)) that reports the corresponding findings across the other diagnostic methods. In this example, among the 67 patients with a positive ipsilateral

Table 1. Number of patients with lateralized primary tumors presenting with a specific configuration of LNL involvement on planning CT. E.g., LI-II means involvement of levels I and II but not III and IV. Ipsi- and contralateral side are reported independently.

Planning CT					
LNL involvement	Oropharynx Ipsi/Ipsi ^a /contra	Oral Cavity Ipsi/Ipsi ^a /contra	Hypopharynx Ipsi/Ipsi ^a /contra	Larynx Ipsi/Ipsi ^a /contra	All Ipsi/Ipsi ^a /contra
None	6/0/39	2/0/6	2/0/16	5/0/7	15/0/68
L I	1/0/1	0/0/0	0/0/1	0/0/0	1/0/2
L II	36/19/25	0/0/2	8/2/3	2/1/2	46/22/32
L III	1/0/0	0/0/0	1/0/1	0/0/0	2/0/1
L IV	0/0/0	1/0/0	0/0/0	0/0/0	1/0/0
L I-II	8/6/3	4/1/1	2/2/3	0/0/0	14/9/7
L I-III	1/1/0	0/0/0	0/0/0	0/0/0	1/1/0
L I-IV	0/0/0	0/0/0	0/0/0	0/0/0	0/0/0
L II-III	15/7/5	0/0/0	8/4/2	2/1/0	25/12/7
L II-IV	0/0/0	0/0/0	0/0/0	0/0/0	0/0/0
L III-IV	0/0/0	0/0/0	0/0/0	0/0/0	0/0/0
L I-II-III	6/4/3	2/2/0	2/1/2	0/0/0	10/7/5
L I-II-IV	0/0/0	0/0/0	0/0/0	0/0/0	0/0/0
L I-III-IV	0/0/0	0/0/0	0/0/0	0/0/0	0/0/0
L II-III-IV	2/0/0	0/0/0	3/2/0	0/0/0	5/2/0
L I-II-III-IV	0/0/0	0/0/0	2/1/0	0/0/0	2/1/0
Total	76/37/76	9/3/9	28/12/28	9/2/9	122/122/54

^acounts the number of patients with the specific ipsilateral involvement configuration plus at least one contralateral LNL involved.

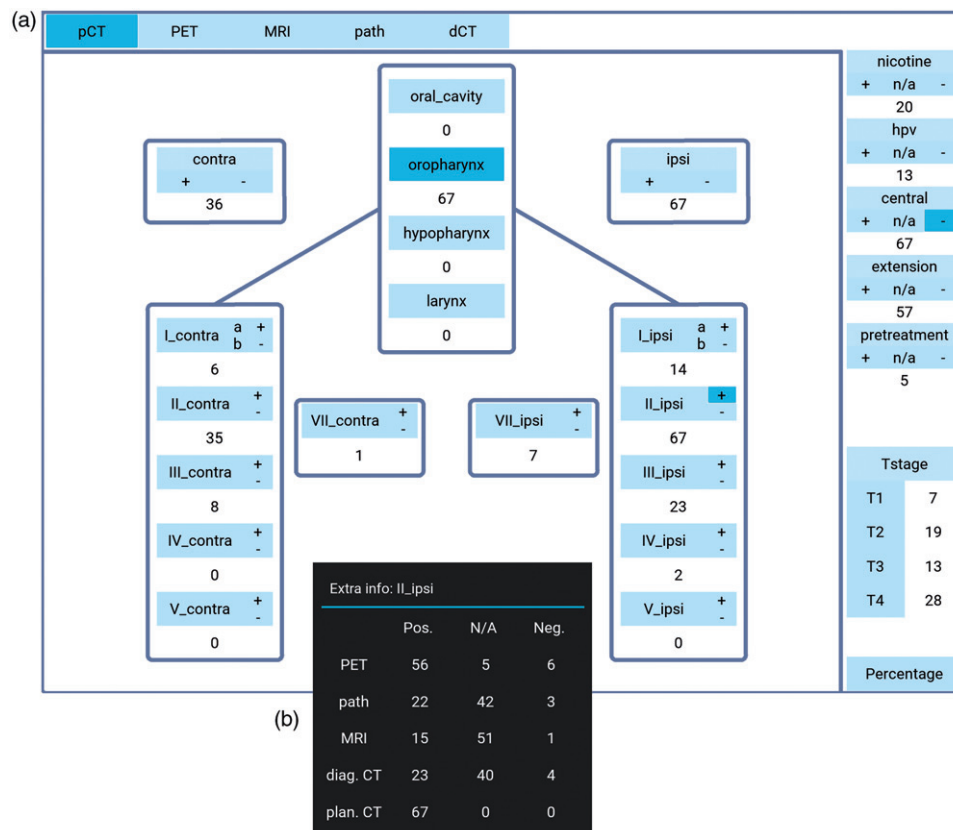


Figure 1. GUI interfacing the SQL database. (a) In the top row, the user selects the diagnostic method under consideration for which LNL involvement is shown. In the right panel, characteristics of the patient and primary tumor can be selected. In the example, only not centrally located tumors are considered. The main panel displays the LNL involvement (see text in Graphical user interface section). (b) By clicking on the LNL button (II ipsi in this example) diagnostic information across all modalities is displayed in an additional window (see text in Graphical user interface section).

involvement of level II on the planning CT, 62 patients had a PET diagnosis available (56 positive, 6 negative for ipsilateral level II) and 5 had no available PET examination. In addition, FNA was performed on level II on 25 patients, confirming metastasis in 22 patients.

Microscopic risk estimation

We apply the method proposed in 'From macroscopic progression patterns to risk of microscopic involvement' section and Appendix B.1 to estimate the risk of microscopic involvement in lateralized oropharyngeal tumors. Our dataset contains 76 such cases in total. Due to this relatively small size, we pool all the cases irrespective of T-stage and other risk factors. The knowledge about lymphatic progression patterns contained in the dataset is mathematically encoded in the so-called likelihood function (equation B7 in Appendix B.1). To calculate the likelihood function, we used the combination of PET (71), diagnostic CT (30) and pathology (27) reported evidence. We specified the specificity and sensitivity (spec./sens.) based on a published meta-analysis [10,11]: (0.86/0.79) for PET, (0.76,0.81) for CT and (0.98/0.8) for Ultrasound guided fine needle aspiration (USgFNA).

To illustrate its use for estimating the risk of microscopic involvement in a new patient, we consider the following scenario. We assume PET as the only diagnostic modality for the new patient and we consider the risk of ipsilateral level

III involvement. To that end, we assume that level III is negative in PET and we distinguish the two cases where level II is positive or negative in PET, respectively. The microscopic risk of involvement in level III for the case of macroscopic metastases in level II is calculated to be 12%. Without evidence of macroscopic metastases in level II, the risk in level III is 9%. The mathematical details are described in Appendix B.2.

Discussion

The general patterns of lymphatic progression are well known and have been described in the literature. However, the number of patients with a specific combination of involved LNL is needed to address the question by how much the observation of metastases in one level affects the risk of microscopic involvement in the residual levels. This, in turn, is needed to personalize CTV-N definition based on a patient's individual state of tumor progression.

In this paper, we make three main contributions to address this problem:

1. We publish a data set of lymphatic progression patterns in 132 HNSCC patients, which is available as [Supplementary Material](#). The dataset is in line with the general patterns of lymphatic progression reported in the literature and the concept of gradual infiltration [4–6]. Level II was involved in the majority of cases while

involvement of level IV was rare (9 cases). Involvement of ipsilateral level III without level II was rare and occurred only twice for lateralized oropharyngeal cases and once for hypopharyngeal cases. Further discussion and a comparison with the values reported in the review by Grégoire et al. [1] are presented in [Appendix A.4](#).

2. The large number of combinations of involved LNL, together with diverse diagnostic methods that are often available for only a subset of patients and LNL, makes it virtually impossible to summarize the information within a paper without substantial loss of relevant information. Therefore, the raw dataset is made available online for consultation. In addition, exploring the dataset is not trivial. To that end, we suggest a data base structure and GUI.
3. We outline how Bayesian statistics can be used to estimate the risk of microscopic involvement from macroscopic progression patterns. Most papers report the percentage of patient's in which a particular LNL harbors metastases. However, this number is very different from the risk of microscopic involvement for a given patient who presents with his or her individual imaging information. For example, in our dataset, ipsilateral level III is macroscopically involved in 23 out of 71 lateralized oropharynx patients, corresponding to 33%. Taking into account the patient's imaging information, the risk in level III is reduced to 12% in the example that level II is positive on PET and level III negative. The difference between these two probabilities is detailed in the [Supplementary materials, Appendix B.2](#).

In conclusion, the decision which lymph node levels (LNL) to include in the CTV-N depends on the risk that LNL harbor microscopic metastases despite negative findings on diagnostic imaging. The methodology presented here may allow for personalized elective CTV definition based on the patient's individual state of tumor progression. However, the collection of larger data sets is required to achieve this goal.

Disclosure statement

The authors report no conflicts of interest.

Funding

This work was supported by the Clinical Research Priority Program of the University of Zurich for the 'Artificial intelligence in Oncological Imaging'.

ORCID

B. Pouymayou  <http://orcid.org/0000-0002-8060-7827>

References

- [1] Grégoire V, Coche E, Cosnard G, et al. Selection and delineation of lymph node target volumes in head and neck conformal radiotherapy. proposal for standardizing terminology and procedure based on the surgical experience. *Radiother Oncol.* 2000;56:135–150.
- [2] Gregoire V, Ang K, Budach W, et al. Delineation of the neck node levels for head and neck tumors: a 2013 update. dahanca, eortc, hknpcsg, ncic ctg, ncri, rtog, trog consensus guidelines. *Radiother Oncol.* 2014;110:172–181. Available from: <https://www.ncbi.nlm.nih.gov/pubmed/24183870>
- [3] Lindberg R. Distribution of cervical lymph node metastases from squamous cell carcinoma of the upper respiratory and digestive tracts. *Cancer.* 1972;29:1446–1449.
- [4] Shah JP, Candela FC, Poddar AK. The patterns of cervical lymph node metastases from squamous carcinoma of the oral cavity. *Cancer.* 1990;66:109–113.
- [5] Candela FC, Kothari K, Shah JP. Patterns of cervical node metastases from squamous carcinoma of the oropharynx and hypopharynx. *Head Neck.* 1990;12:197–203.
- [6] Sanguineti G, Califano J, Stafford E, et al. Defining the risk of involvement for each neck nodal level in patients with early t-stage node-positive oropharyngeal carcinoma. *Int J Radiat Oncol Biol Phys.* 2009;74:1356–1364. Available from: <https://www.ncbi.nlm.nih.gov/pubmed/19131181>
- [7] Pearl J. Probabilistic inference in intelligent systems. Burlington (MA): Morgan Kaufmann; 1988.
- [8] Darwiche A. Modeling and reasoning with bayesian networks. Cambridge: Cambridge University Press; 2009.
- [9] Bertrand P, Panagiotis B, Oliver R, et al. A bayesian network model of lymphatic tumor progression for personalized elective ctv definition in head and neck cancer. *Phys Med Biol.* 2019. Available from: <http://iopscience.iop.org/10.1088/1361-6560/ab2a18>.
- [10] De Bondt R, Nelemans P, Hofman P, et al. Detection of lymph node metastases in head and neck cancer: a meta-analysis comparing us, usgfnac, ct and mr imaging. *Eur J Radiol.* 2007;64:266–272.
- [11] Kyzas PA, Evangelou E, Denaxa-Kyza D, et al. 18f-fluorodeoxyglucose positron emission tomography to evaluate cervical node metastases in patients with head and neck squamous cell carcinoma: a meta-analysis. *J Natl Cancer Inst.* 2008;100:712–720.